

Truss-arch model for shear strength of seismic-damaged SRC frame columns strengthened with CFRP sheets

Sheng PENG^{a*}, Chengxiang XU^a, Xiaoqiang LIU^{a,b}

^a Department of Civil Engineering, Wuhan University of Science and Technology, Wuhan 430065, China

^b School of Architectural Engineering, Weifang University of Science and Technology, Weifang 262700, China

*Corresponding author. E-mails: pe_sh@sina.com; pengsheng@wust.edu.cn

© Higher Education Press and Springer-Verlag GmbH Germany, part of Springer Nature 2019

ABSTRACT Carbon fiber reinforced polymer (CFRP) materials are important reinforcing substances which are widely used in the shear strengthening of seismic-damage steel reinforced concrete (SRC) frame structures. To investigate the shear strength of SRC frame columns strengthened with CFRP sheets, experimental observations on eight seismic-damaged SRC frame columns strengthened with CFRP sheets were conducted at Yangtze University and existing experimental data of 49 SRC columns are presented. Based on the existing experiments, the theories of damage degree, zoning analysis of concrete, and strengthening material of the column are adopted. To present the expression formula of the shear strength of SRC frame columns strengthened with CFRP sheets, the contributions of strengthening material and transverse reinforcement to shear strength in the truss model are considered, based on the truss-arch model. The contribution of arch action is also considered through the analysis of the whole concrete and that of the three zones of the concrete are also considered. The formula is verified, and the calculated results are found to match well with the experimental results. Results indicate that the proposed whole analysis model can improve the accuracy of shear strength predictions of shear seismic-damaged SRC frame columns reinforced with CFRP sheets.

KEYWORDS carbon fiber reinforced polymer material, steel reinforced concrete frame column, seismic-damaged, trussed-arch model, shear strength

1 Introduction

A large number of existing seismic-damaged steel reinforced concrete (SRC) columns at different levels of seismicities are not included in guideline publications, and cannot be strengthened according to the requirements of modern seismic design codes [1]. If vital deficiencies in such columns, which are generally called seismic-damaged SRC columns, the related strength analysis strengthening materials and initially damaged degrees had to be considered [2]. Recent post-earthquake investigations have indicated that after being strengthened, seismic-damaged SRC columns are vulnerable to shear failure as one of the main load-bearing parts. This results in a rapid reduction of seismic performance, and often leads to easy structural collapse during earthquakes [3–5]. To satisfy the aseismic requirements of seismic-damaged SRC struc-

tures, the brittle shear failure mode must be avoided. In practical engineering, carbon fiber reinforced polymer (CFRP) has received considerable attention due to factors including its high-strength, light weight, high corrosion resistance, and ease of fabrication. This effective strengthening method for SRC structures is increasingly used in the United States, Canada, Japan, and more recently in Europe. To mitigate brittle shear failure under the action of an earthquake, a more thorough assessment of seismic-damaged SRC columns strengthened with CFRP is required [6–10]. Meanwhile, in order to sustain the new or improved concrete structures in an earthquake, strengthened columns must be designed with enough shear strength as it is one of the main load-bearing components of the building structure.

Compared to normal concrete columns, seismic-damaged reinforced concrete (RC) columns strengthened with CFRP demonstrate a different seismic performance and are more brittle under the same conditions, leading to a

limited application in all aseismatics design [11–15]. In light of this, research into the seismic performance of the seismic-damaged RC columns strengthened with CFRP has increased dramatically in recent years in order to standardize the use of CFRP-strengthened concrete structures in seismicity regions. Fukuyama et al. [16] studied the shear bearing capacity and ductility of seismic-damaged RC columns strengthened with CFRP subjected to a constant axial load and cyclic lateral loads. Cai [17] investigated the seismic performance of CFS-strengthened RC short columns based on the test phenomenon and results, presenting formulas for computing the shear-strength of columns. Eight RC columns with smaller ductility were tested by Iacobucci under cyclic loading, and the effect of the seismic-damaged RC columns strengthened with CFRP was investigated on the performance of the columns [18]. Through analyzing the data from numerous column tests, Sezen and Moehle [19] obtained the parameters affecting the shear-strength of RC columns of a rectangular cross-section and light transverse reinforcement. Wang et al. [20] studied RC structure under different degrees of seismic damage and when strengthened with CFRP, and analyzing the seismic behavior of the RC structure. Wang [21] tested four seismic-damaged RC columns strengthened with CFRP and examined the difference in behavior between strengthened RC columns and normal RC columns. Zhao and Ye [22] carried out an experiment to investigate the seismic behavior of the strengthened columns, finding that shear-strength was improved and brittle failure was avoided effectively. Zhang et al. [23] studied the shear bearing capacity and seismic behavior of four severely damaged RC columns strengthened with CFRP sheets subjected to a constant axial load and cyclic lateral loads. Zhou et al. [24] summarized that the seismic performance of the rehabilitated columns could reach or even exceed that of the original columns before seismic damage within a certain extent of damage level. Pan and Li [25] summarized a series of experiments on the shear behavior of RC components and developed a shear strength equation as a function of inelastic deformation. Jin et al. [26] tested eight columns with high strength steel and concrete under axial compression load and cyclic loading. They concluded that the shear strength equation provided by Pan et al. was conservative for high-strength columns, and proposed modifications to the detailed shear strength equation proposed by Pan. Ichinose [27] presented an expressive formula for the shear strength of an RC frame column strengthened with CFRP sheets based on the truss-arch model.

Existing studies primarily focus on the shear behavior of seismic-damaged RC columns strengthened with CFRP under simulated earthquake loading, while less information can be obtained on the shear performance of seismic-damaged SRC columns strengthened with CFRP. Recent post-earthquake reconnaissance has indicated that some short SRC columns or SRC columns without seismic

damage are vulnerable to shear failure, which will drastically reduce structural seismic performance and usually lead to structural collapse during earthquakes. The most important aspect to this study is the shear behavior of the seismic-damaged SRC columns strengthened with CFRP sheets under constant axial-load and cyclic lateral loads. Thus, the shear strength of the seismic-damaged SRC columns strengthened with CFRP is investigated in this paper. The shear bearing capacity of RC in the specimen is composed of contributions from concrete and transverse reinforcement in many codes which contain some empirical coefficients mostly drawn from experiments performed on normal-strength concrete, respectively. As a result, the applicability of the existing shear design methods of seismic-damaged SRC columns strengthened with CFRP sheets in the specimen must be further evaluated.

This paper presents experimental data on eight strengthened seismic-damaged SRC frame columns which were tested by Yangtze University, as well as simulation data of four specimens from Ref. [2]. The shear span ratio, λ , and the axial-load ratio, n , have an influence on the shear strength of specimens, and Ichinose's shear model reflects this effect. To accurately the influence of damage degree, division zone of concrete, and CFRP material on the truss-arch model, Ichinose's shear model must be improved. To validate the proposed model, test data of eight strengthened seismic-damaged SRC columns and simulation data of four strengthened seismic-damaged SRC columns are collected and compared with design codes.

2 Research significance

To understand the behavior of strengthening seismic-damaged SRC frame columns, a comprehensive experimental program is conducted in which the two main objectives are planned simultaneously. The first objective is to make direct comparisons of the seismic behavior of specimens with two different influence parameters. The second objective is to present a truss-arch model and evaluate the applicability and effectiveness of five different shear-strength models.

3 Observed experimental results

Arch action is significant in seismic-damaged SRC frame columns strengthened with CFRP sheets that have been subjected to the combined action of lateral cyclic loading and axial compressive loading. Jin et al. [26] has proposed that shear failure and flexural-shear failure are both regarded as shear failure. The effect of axial compressive loading on shear strength includes three aspects: first, the compressive force can increase the neutral axis depth of the section; secondly, the angle of the slanting crack is

reduced; and thirdly, with the decrease of crack width, the ability of the crack interface to transmit shear force is enhanced [26]. The arch action can represent the first aspect, and the truss model can represent the other two aspects.

3.1 Experimental observation at Civil Engineering Experiment Center of Yangtze University

Four SRC columns with different degrees of post-earthquake damage were designed and numbered from SRC-1 to SRC-4 for the test. The columns were studied to examine the shear strength of SRC columns strengthened with CFRP sheets. Four other SRC columns with different axial-load ratios were also designed for the experiment, and numbered from SRCC-2 to SRCC-4. The testing was then undertaken at the Civil Engineering Experiment Center of Yangtze University, China, with the experiment and simulation conducted by Peng et al. [2]. To simulate an earthquake situation, specimens were tested under a combination of cyclic shear force and a constant axial load. The main parameters included shear span ratio, λ , post-earthquake damage degree, strengthening methods, and the axial-load ratio, n . Figure 1 shows the experimental parameters of the specimen, and Table 1 presents the dimension and strengthening material of the specimen. The axis load on the top of the specimen was applied slowly until the design value and then remained constant. Peng et al. were consulted regarding details of the test device and loading system [1,2].

The diameter of longitudinal reinforcement was 16 mm, and the yield strength of longitudinal reinforcement, f_{ck} , was 376 MPa. The diameter of stirrups was 8 mm, and the yield strength of stirrups, f_{vy} , was 312 MPa. The spacing between stirrups, s , was 200 mm and the 10-16# I-beam was constructed at the core of the column section. The cross-section reinforcement ratio (ρ_l) of the specimens was 1.60%, the stirrup ratio (ρ_v) was 0.68%, and steel ratio (ρ_a) of the specimens was 4.84%.

The SRC column base was strengthened with CFRP sheets. The CFRP sheets with a tensile stress of $f_{st} = 3560$ MPa and an elastic modulus of $E = 250000$ MPa were pasted in a direction perpendicular to the axis of the column using the circular uniform packing method. The

layer number was two, the monolayer thickness, t_{st} , was 0.111 mm, the elongation was 1.7%, lap length was 150 mm, and the strengthening height was 500 mm. To ensure the same quality of concrete, the same batch of C40 commercial concrete was used. The 28 day average compressive cylinder strength was 37.2 MPa, while the cylinder strength was 39.6 MPa at the time of the actual test (GB 50010 2010). The average compressive strength of testing for each specimen is summarized in Table 1. More details of the specimens can be found in Refs. [1,2].

The backbone curves of the SRC-1–SRC-4 and SRCC-2–SRCC-4 series of specimens are illustrated in Fig. 2. The stress process of the specimens are made up of four stages being elasticity, elasticity and plasticity, yielding and failure. Shear failure of the tested column is defined as the recorded shear force when the shear strength decreases to 85% of the maximum shear capacity or the column is unstable and cannot continue to work.

As seen in Fig. 2, compared with specimen SRC-1, the shear strength of specimen SRC-2 is increased by 12.39%, that of specimen SRC-3 is increased by 9.13%, and that of specimen SRC-4 is increased by 8.76%. As the damage degree decreases, the arch action of seismic-damaged SRC frame columns, which were strengthened with CFRP sheets, distinctly increases.

3.2 Material damage description and hypothesis

Post-earthquake damage of the tested columns is called strength reduction, and is described by the strength reduction factor, a_F [28,29]. The expression for a_F is as follows:

$$a_F = 1 + \beta_1 D + \beta_2 D^2, \quad (1)$$

where D is the damage index of a specimen, which was proposed by Zheng et al. [30]. The correlation coefficients are β_1 and β_2 , and can be computed by Eqs. (2a) and (2b), respectively.

$$\beta_1 = 0.127 - 0.000586f'_{yv} + 0.229 \left(\frac{f'_{yv}}{1000} \right)^2 + 0.00143f_c, \quad (2a)$$

Table 1 Specimens experimental parameters

specimen	damage degree	n	λ	concrete strength grade	CFRP layer number	strengthened	$\mu = \Delta_u/\Delta_y$	$V_{u,t}$ (kN)
SRC-1	undamaged	0.32	3.33	C40	–	no	2.87	127.07
SRCC-2	undamaged	0.20	3.33	C40	–	no	3.12	112.52
SRCC-3	undamaged	0.40	3.33	C40	–	no	2.47	130.44
SRCC-4	undamaged	0.60	3.33	C40	–	no	1.89	132.89
SRC-2	undamaged	0.32	3.33	C40	2	yes	3.38	151.60
SRC-3	moderate damaged	0.32	3.33	C40	2	yes	3.26	144.45
SRC-4	severe damaged	0.32	3.33	C40	2	yes	3.12	140.11

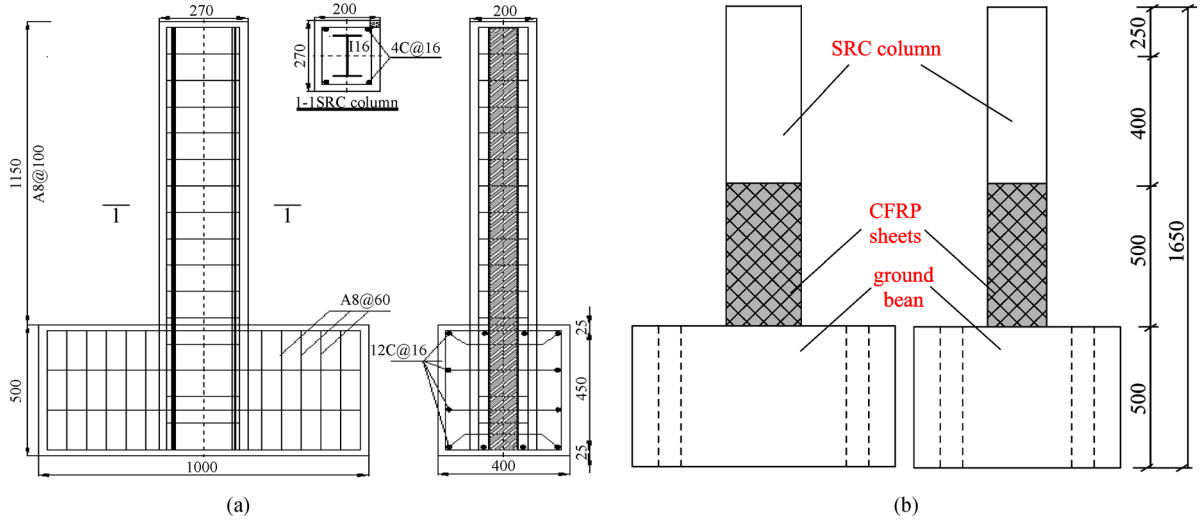


Fig. 1 Specimen dimension and strengthening (unit: mm). (a) Geometry and steel reinforcement configuration for specimens; (b) strengthening of CFRP sheets at column bottom.

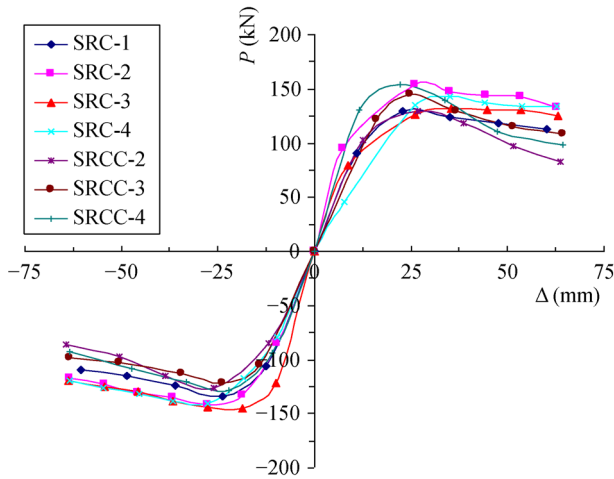


Fig. 2 Skeleton curves of specimens.

$$\beta_2 = -1.013 + 0.585n - 1.762n^2 + 0.183\rho_a + \frac{10.959}{f_c} \quad (2b)$$

A simplified method to calculate the strength of the stirrups, longitudinal bars, and section steel after earthquake damage is presented in Eq. (3c). Similar observations were also reported by Yang [28].

$$f'_{yv} = a_E f_{yv}, \quad (3a)$$

$$f'_{ck} = a_E f_{ck}, \quad (3b)$$

$$f'_a = a_E f_a, \quad (3c)$$

where f_{yv} , f_{ck} , f_a is the original strength of stirrups, longitudinal bars and section steel of test columns without

initial seismic damage, respectively; and f'_{yv} , f'_{ck} , f'_a is the strength of the stirrups, longitudinal bars and section steel of test columns under existing initial seismic damage, respectively.

There are no research results or reliable methods for estimating the change of the non-core-zone area of the section column. Zhao and Cao [31] suggested that the area of RC column could be simplified as bh . Based on test results by Lu [32], Wan [33], and Zhang [34], the area of the post-earthquake damage columns is not equal to bh .

From Fig. 3(a), it can be seen that the column section consists of two parts with stirrups as boundaries: core zone area, A_1 , and non-core-zone area, A_2 . These can be computed by Eqs. (4a) and (4b), respectively.

$$A_1 = 2b(h - a_s), \quad (4a)$$

$$A_2 = (h - 2a_s)(b - 2a_s). \quad (4b)$$

The column cross-section area, A , is expressed as:

$$A = (1 - D_1)A_1 + a_F A_2, \quad (5)$$

where D_1 is the damage index of the non-core-zone area of the section column: D_1 is equal to 0.5 for moderate damage and D_1 is equal to 1.0 for severe damage.

Yang [28] and Zhao and Cao [31] provided a simplified method to calculate the effective area, A_e , of the compression strut on the concrete calculated. These results are presented in Fig. 4.

$$A_e = \begin{cases} bh \left(1 - \frac{\pi b}{8h}\right), & (6a) \\ bh \left(1 - \frac{b}{4h}\right). & (6b) \end{cases}$$

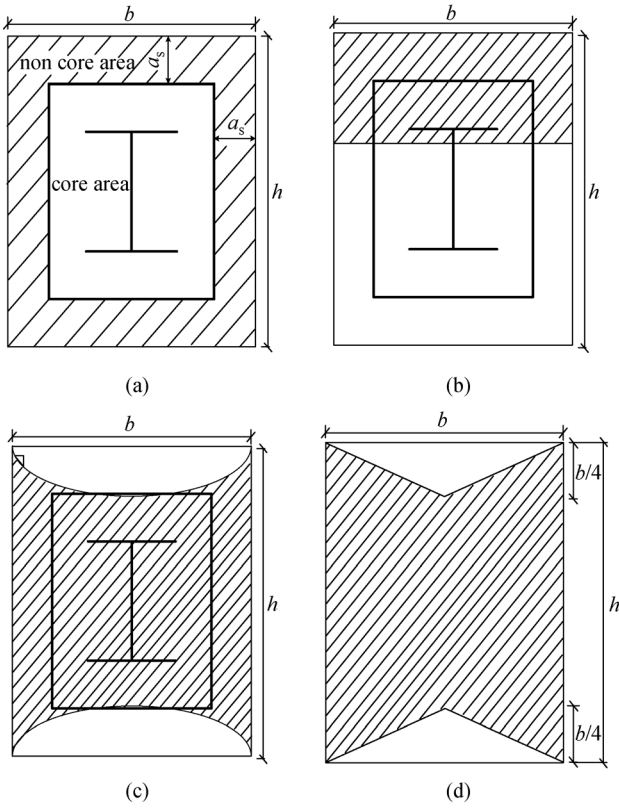


Fig. 3 Geometric dimension and compression zone. (a) Column cross-section; (b) compression zone; (c) compression zone of inclined cracks region; (d) simplify the compression zone of inclined cracks region.

From Fig. 4, Eq. (6) is non conservative however, the mean is comparatively conservative. To facilitate the calculation, it is assumed that the column section height h , does not change, and expressed as:

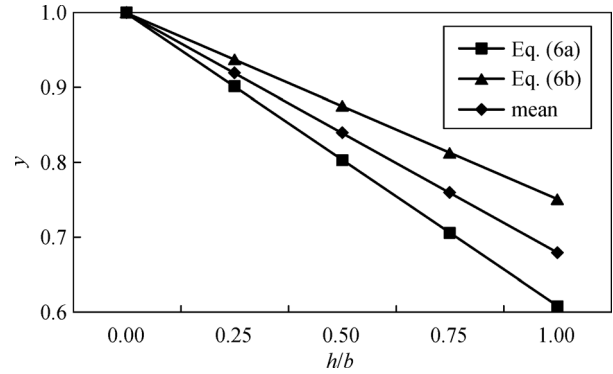


Fig. 4 Comparison of effective area formula.

$$A_e = \frac{1}{2} \left[bh \left(1 - \frac{\pi b}{8h} \right) + bh \left(1 - \frac{b}{4h} \right) \right] = bh \left[1 - \frac{(\pi + 2)b}{16h} \right]. \quad (7)$$

3.3 Steel component

In Eq. (8), the shear bearing capacity of the component steel section is considered regarding pure shear which is also accepted in GB50010-2010 [35].

$$V_a = \frac{0.58f'_a t_w h_w}{\lambda - 0.2}. \quad (8)$$

3.4 Truss component

From Fig. 5, the concrete contribution to shear strength in the truss model, V_t , is assumed as the amount of force transferred across the constrain interface of transverse stirrups and CFRP sheets.

V_t is expressed as

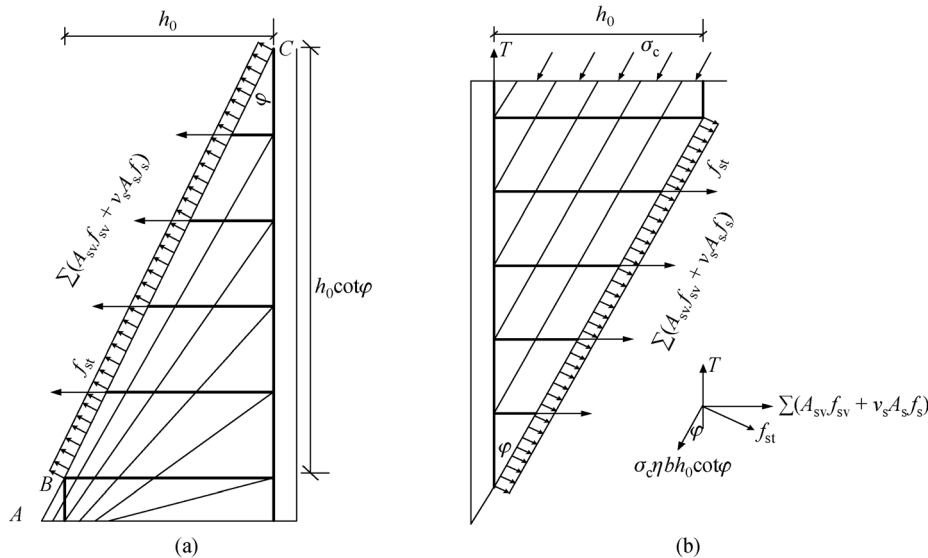


Fig. 5 The truss model. (a) Balance of truss model force; (b) balance of isolated-body force.

$$V_t = (f'_{yv}\rho_{sv} + v_s f'_{st}) \cdot 0.9b_1(h - 2a_s)\cot\varphi. \quad (9)$$

To calculate the value of $\cot\varphi$, a simplified method is provided as follows:

$$\cot\varphi = \min \left\{ \sqrt{\frac{\eta v f_c}{\rho_{sv} f'_{yv} + v_s f'_{st}} - 1}, 2 \right\}. \quad (10)$$

In Fig. 5(b), the stirrups reach the limit state, and the oblique compressive stress, σ_c , of the concrete in the truss model is expressed as

$$\sigma_c = \frac{f'_{yv}\rho_{sv} + v_s f'_{st}}{\eta \sin^2\varphi}, \quad (11)$$

where η is the influence coefficient of constraint action of stirrups on strengthening considered in the truss model, and can be calculated by Eq. (12); f'_{st} is the tensile strength of strengthening materials, MPa; φ is the angle between the compression concrete and the column axis in the truss model (also called critical shear angle); ρ_{sv} is the reinforcement ratio of stirrups, and v_s is the shear coefficient of reinforced material.

$$\eta = 1 - [(\pi + 2)b/16h]. \quad (12)$$

3.5 Arch component

The arch action indicates that the compressive force can increase the neutral axis depth of the section (Fig. 6). If the arch pressure is mainly concentrated in the central part of the arch model, the whole analysis of the concrete with column section is carried out, as illustrated in Fig. 6(b). If

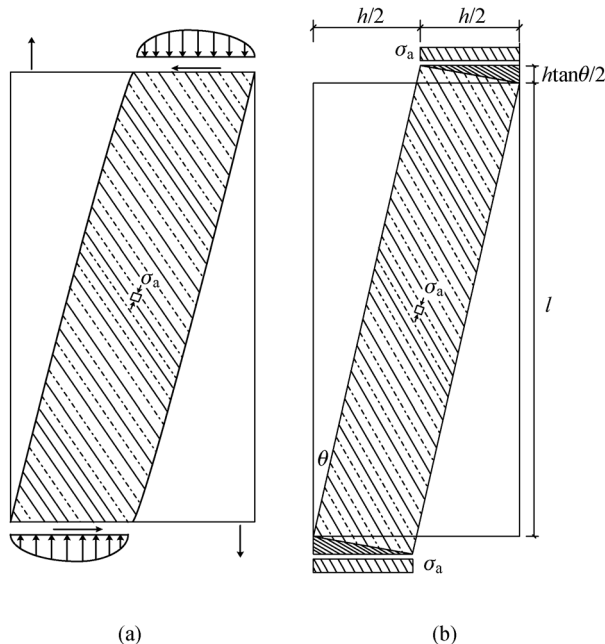


Fig. 6 The arch model. (a) The actual arch model; (b) the simplified arch model.

the effect of the column section on the concrete of the arch model is being considered, the analysis of the concrete with column section is divided into three zones (Fig. 7). Wei and Zhang [36] individually tested three zones: the outer and left sides without flange and web restraint, the upper and lower zones of the flange, and the restricted flange inboard zone.

There are similarities to the arch action of the two models, however, Zhao and Cao's model requires the analysis of the concrete as a whole, whereas Wei and Zhang's model considers the zones individually. Examining the mechanical properties of steel is the main method to study the contribution of the arch mechanism to shear strength. Neither models examine the difference of shear strength in the arch model between the analysis of the whole concrete and that of the concrete divided into three zones [31,36]. To obtain the arch contribution, the condition of compatibility between the concrete and the strengthening material must be derived.

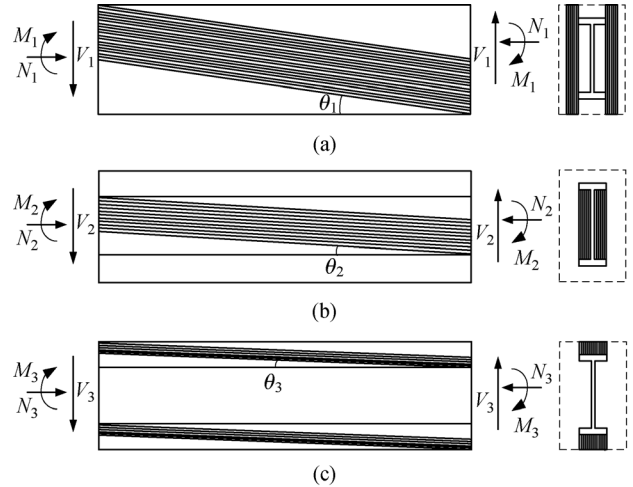


Fig. 7 Arch model graph of RC part in SRC short column. (a) The outer and left sides without flange and web restraint; (b) the upper and lower zones of the flange; (c) the restricted flange inboard zone.

Shear deformation of the arch model results in shear deformation of the truss model. The shear failure criterion of the truss-arch model can be expressed as:

$$\sigma_c + \alpha\sigma_a = v f_c, \quad (13)$$

where v is the softening coefficient of concrete and can be computed by Eq. (14). When v is less than 0.4, the term v can be simply taken as 0.4, and α is the effective coefficient of the arch model.

$$v = 0.75 - f_c/170. \quad (14)$$

As seen in Fig. 6(b), the effect of the arch model on the shear strength of concrete, V_{a1} , is assumed to be the whole analysis of the concrete with a RC column section. The contribution of concrete to shear can be expressed as:

$$V_{a1} = \sigma_a \frac{b_1 h^2}{4}, \quad (15)$$

where the arch pressure, σ_a , of concrete in the arch model consists of the arch pressure produced by the axial load, σ_{a0} , and the arch pressure produced by the shear, σ_{aN} .

To calculate the value of σ_{a0} and σ_{aN} , similar observations provide a simplified method [22].

$$\sigma_a = \sigma_{a0} + \sigma_{aN}, \quad (16)$$

where

$$\sigma_{a0} = \begin{cases} \gamma f_c, & \lambda \leq 0.5 \\ (1.2 - 0.4\lambda) \cdot \gamma f_c, & 0.5 < \lambda < 3 \\ 0, & \lambda \geq 3 \end{cases}$$

$$\sigma_{aN} = 2n f_c.$$

From Fig. 7, the shear strength, V_{a2} , of the RC column consisting of three zones is as follows:

$$V_{a2} = V_1 + V_2 + V_3, \quad (17)$$

where

$$V_1 = (1 - \beta) \gamma f_c \frac{b_1 h}{2} \tan \theta_1,$$

$$V_2 = (1 - \beta) \gamma f_c \frac{(b_f - t_w) h_w}{2} \tan \theta_2,$$

$$V_3 = (1 - \beta) \gamma f_c \frac{b_f (h - h_w - 2t_w)}{2} \tan \theta_3,$$

where

$$\beta = (1/\eta) \rho_v f_{yv} (1 + \cot^2 \varphi) / (\gamma f_c),$$

$$\tan \theta_1 = h / (2l),$$

$$\tan \theta_2 = h_w / (2l),$$

$$\tan \theta_3 = (h - h_w - 2t_w) / (2l),$$

$$h_w = h_1 - 2d_f,$$

$$\gamma = f_c / 165.$$

Equation (17) is put forward by Zhang [34]. The high cross section of the I-beam is h_1 . b_f is the width of the flange of the I-beam section; d_f is the thickness of the I-beam flange, and t_w is the thickness of the I-beam web.

3.6 Shear coefficient analysis

The contribution of CFRP to shear in the truss-arch model

is based on modified strength degradation. The contribution of CFRP to shear can be expressed as:

$$v_s = \alpha_{\text{CFRP}} v_{\text{CFRP}}, \quad (18)$$

where α_{CFRP} is CFRP strength reduction factor and can be computed by Eq. (19) [37], and v_{CFRP} is the CFRP strength effective coefficient and can be computed by Eq. (20) [28].

$$\alpha_{\text{CFRP}} = \frac{1.639}{\sqrt{(t_{\text{st}} b_{\text{st}} f_{\text{st}}) / (b_1 s_{\text{st}} f_t) + 1.207}}, \quad (19)$$

$$v_{\text{CFRP}} = 0.27 + 0.09\lambda - 0.13n, \quad (20)$$

where t_{st} is thickness and b_{st} is width of CFRP for calculating α_{CFRP} , and s_{st} is 1 for CFRP spacing. b_1 is the effective width of column, and $b_1 = b - 2a_s$. Therefore, the shear strength of seismic-damaged SRC columns strengthened with CFRP sheets under cyclic reversed loading is:

$$V_{u1} = V_a + V_t + V_{a1} = \frac{0.58 f'_a t_w h_w}{\lambda - 0.2} + (f'_{yv} \rho_{sv} + v_s f_{\text{st}}) \cdot 0.9 b_1 (h - 2a_s) \cos \varphi + \frac{b_1 h^2}{4} (\sigma_{a0} + \sigma_{aN}), \quad (21a)$$

$$V_{u2} = V_a + V_t + V_{a2} = \frac{0.58 f'_a t_w h_w}{\lambda - 0.2} + (f'_{yv} \rho_{sv} + v_s f_{\text{st}}) \cdot 0.9 b_1 (h - 2a_s) \cos \varphi + (V_1 + V_2 + V_3). \quad (21b)$$

4 Evaluation of proposed model

4.1 Experimental verification using test results at Yangtze University

Table 2 logs the ratio of measured shear strength for the proposed model and models of GB 50010-2010, ACI 318-08, and CSA-04 to calculated ones [35,38,39]. This proposed model consisted of two situations: the shear strength, V_{u1} , of the whole analysis and the shear strength, V_{u2} , of the three zones analysis. The mean ratio is 1.148, 1.458, 1.949, 1.164, and 1.076 for the proposed model (V_{u1} and V_{u2} , respectively), GB 50010-2010, ACI 318-08, and CSA-04, respectively. Its coefficient of variation is 0.006, 0.030, 0.020, 0.004, 0.002 for the proposed model (V_{u1} and V_{u2} , respectively), and GB 50010-2010, ACI 318-08, and CSA-04, respectively.

Results show that the proposed model slightly underestimates the shear strength, but can still describe the shear strength well. The proposed model of shear strength, V_{u2} , of the three zones analysis model also demonstrates good calculation precision. For the columns, the ratio of the test value to the theoretical calculation value is more than 1.0, that is to say, the proposed method is safe in practical

Table 2 Comparisons of shear strength between proposed model and other models

specimen	a_F	λ	n	V_e/V_{GB}	V_e/V_{ACI}	V_e/V_{CSA}	proposed model	
							V_e/V_{u1}	V_e/V_{u2}
SRC-1	1.00	3.33	0.32	1.081	1.382	1.898	1.108	1.028
SRCC-2	1.00	3.33	0.20	1.102	1.365	1.856	1.112	1.065
SRCC-3	1.00	3.33	0.40	1.128	1.406	1.874	1.128	1.088
SRCC-4	1.00	3.33	0.60	1.043	1.412	1.928	1.119	1.009
SRC-2	1.00	3.33	0.32	1.312	1.965	2.056	1.312	1.165
SRC-3	0.96	3.33	0.32	1.228	1.386	2.354	1.228	1.092
SRC-4	0.89	3.33	0.32	1.143	1.292	1.678	1.143	1.086
mean				1.148	1.458	1.949	1.164	1.076
coefficient of variation				0.006	0.030	0.020	0.004	0.002

engineering.

From Table 2 it can be seen that the predicted shear strength of the GB 50010-2010 model and the proposed whole analysis model are approximately equal as the columns at the Civil Engineering Experiment Center of Yangtze University are designed and manufactured according to the national code GB 50010-2010. Because the influence of damage degree is considered in the proposed model, the calculated shear strength decreases as the damage degree increases.

4.2 Evaluation of proposed model 49 SRC columns

To investigate the shear strength of SRC frame columns strengthened with CFRP sheets, existing experimental data of 49 SRC columns are presented and summarized in Table 3.

A compiled experimental database of 53 SRC columns was used to evaluate the popular models from GB 50010-2010, ACI 318-08, CSA-04, and the proposed model. The proposed model is made up of the whole analysis model and the three zones analysis model. The database consists of four columns tested at Yangtze University and 49 columns in the aforementioned literature. Figures 8–10 plot the ratio of measured shear strength, V_e , to the calculated shear strengths V_{u1} , V_{u2} , V_{GB} , V_{ACI} , and V_{CSA} , versus the shear span ratio, axial-load ratio, and strength reduction factor, respectively. Through analysis of the data, the proposed model can reasonably predict the shear strength.

The mean ratio of test value to calculate value shear strength is 1.214, 1.558, 2.363, 1.257, and 1.076, respectively. The coefficient of variation is 0.004, 0.179, 0.090, 0.005, and 0.002, respectively. The proposed model calculating the shear strength of the SRC column is conservative and compared to the whole analysis model, the three zones analysis model displays the best precision. There are two major reasons that account for the differences. First, in the proposed truss-arch model, the

effective depth of the arch can be obtained by the depth of the neutral axis of the section minus the thickness of the concrete cover. However, in some tested columns, the concrete cover did not spall at the shear failure and so the arch action was underestimated. Secondly, the proposed V_{u2} in Eq. (21b) is concerned with the shear strength of the steel section of the concrete and it is safe for practical application.

From the results of the comparison, there is a risk of overestimating the shear strength using the model of the CSA-04 method which has been approved by GB 50010-2010. Using the ACI 318-08 method, the predicted shear strength of the database is generally conservative, however, the value is underestimated for smaller λ and overestimated for larger λ . The main cause of this difference is that the arching effect decreases with the increase of shear span ratio, λ . The CSA-04 model is based on the MCFT, which can also predict the shear strength relatively accurately. Because the influence of the arch model is not considered in the CSA-04 model, for columns with $\lambda < 2.5$, the predicted shear strength is slightly conservative.

5 Summary and conclusions

Test results and analysis of 53 SRC columns illustrated that shear span ratio and axle-load ratio had a significant effect on the shear strength of the specimens. Shear strength of SRC columns is mainly transferred by the truss mechanism and the arch action. Based on the condition of deformation compatibility between the truss model and the arch model, a predictive expression for shear strength of SRC columns was presented under low cyclic loading. The influence of damage degree and confinement method on the truss-arch mechanism was then considered.

By comparing the experimental values and calculated values of the shear strength of 53 SRC columns, it was found that shear strength of the proposed model displayed

Table 3 Parameters of 49 SRC columns

specimen	reference	a_F	λ	n	f_c (MPa)	$b \times h$ (mm ^{2.0})	L (mm)	ρ_a	f_a (MPa)	ρ_{sv}	f_{yv} (MPa)	f_{st} (MPa)	t_{st} (mm)	b_{st} (mm)	I^*	V_c (kN)
SRC-1	[21]	1	1.0	0.36	66.4	200 × 160	370	6.11	261.6	0.8	462.6	–	–	–	I14	371.6
SRC-2		1	1.0	0.36	67.3	200 × 160	480	6.11	261.6	1.2	354.5	–	–	–	I14	395.3
SRC-3		1	1.0	0.36	70.4	200 × 160	480	6.11	261.6	1.6	354.5	–	–	–	I14	424.2
SRC-4		1	1.5	0.36	66.4	200 × 160	480	6.11	261.6	0.8	462.6	–	–	–	I14	282.6
SRC-5		1	1.5	0.36	67.3	200 × 160	480	6.11	261.6	1.2	354.5	–	–	–	I14	292.8
SRC-6		1	1.5	0.36	70.4	200 × 160	480	6.11	261.6	1.6	354.5	–	–	–	I14	315.4
SRC-7		1	2.50	0.36	66.4	200 × 160	700	6.11	261.6	0.8	462.6	–	–	–	I14	189.7
SRC-8		1	2.50	0.36	65.3	200 × 160	700	6.11	261.6	1.2	354.5	–	–	–	I14	193.9
SRC-9		1	2.50	0.36	73.1	200 × 160	700	6.11	261.6	1.6	354.5	–	–	–	I14	198.1
SRC-10		1	2.0	0.20	81.8	200 × 160	590	6.11	261.6	0.8	462.6	–	–	–	I14	195.7
SRC-11		1	2.0	0.20	81.8	200 × 160	590	6.11	261.6	1.2	354.5	–	–	–	I14	205.7
SRC-12		1	2.0	0.20	83.1	200 × 160	590	6.11	261.6	1.6	354.5	–	–	–	I14	212.1
SRC-13		1	2.0	0.28	83.1	200 × 160	590	6.11	261.6	0.8	462.6	–	–	–	I14	228.8
SRC-14		1	2.0	0.28	81.8	200 × 160	590	6.11	261.6	1.2	354.5	–	–	–	I14	232.6
SRC-15		1	2.0	0.28	84.9	200 × 160	590	6.11	261.6	1.6	354.5	–	–	–	I14	241.5
SRC-16		1	2.0	0.36	84.9	200 × 160	590	6.11	261.6	0.8	462.6	–	–	–	I14	237.7
SRC-17		1	2.0	0.36	84.4	200 × 160	590	6.11	261.6	1.2	354.5	–	–	–	I14	242.7
SRC-18		1	2.0	0.36	84.4	200 × 160	590	6.11	261.6	1.6	354.5	–	–	–	I14	249.1
SRC-19		1	1.0	0.36	84.4	200 × 160	590	6.11	261.6	1.2	354.5	–	–	–	I14	473.8
SRC-20		1	1.5	0.36	84.9	200 × 160	590	6.11	261.6	1.6	354.5	–	–	–	I14	371.6
SRC1	[28]	1	2.75	0.15	25.9	300 × 300	825	4.53	309.6	1.19	513.4	–	–	–	I20a	245
SRC2		1	2.75	0.30	25.9	300 × 300	825	4.53	309.6	1.19	513.4	–	–	–	I20a	251
SRC3		1	2.75	0.40	25.9	300 × 300	825	4.53	309.6	1.19	513.4	–	–	–	I20a	275
SRC4		1	2.75	0.30	29	300 × 300	825	4.53	309.6	1.19	513.4	–	–	–	I20a	275
SRC5		1	2.75	0.30	29	300 × 300	825	4.53	309.6	1.19	513.4	–	–	–	I20a	255
SRC6		1	2.75	0.45	29	300 × 300	825	4.53	309.6	1.19	513.4	–	–	–	I20a	296
SRC7		1	2.50	0.30	34.3	300 × 300	825	3.95	309.6	1.55	513.4	–	–	–	I20a	270
SRC8		1	2.50	0.30	34.3	300 × 300	825	3.95	309.6	2.42	466.1	–	–	–	I20a	226
SRC9		1	2.50	0.30	34.3	300 × 300	825	3.95	309.6	1.61	466.1	–	–	–	I20a	266
SRC10		1	2.50	0.30	34.3	300 × 300	825	3.95	309.6	2.27	466.1	–	–	–	I20a	287
SRC11		1	2.50	0.30	34.3	300 × 300	825	3.95	309.6	1.61	466.1	–	–	–	I20a	260
SRC12		1	2.50	0.30	34.3	300 × 300	825	3.95	309.6	1.61	466.1	–	–	–	I20a	278
SRC13		1	2.25	0.30	34.3	300 × 300	825	3.95	309.6	1.61	466.1	–	–	–	I20a	304
SRC14		1	2.25	0.30	34.3	300 × 300	825	3.95	309.6	1.55	466.1	–	–	–	I20a	312
SRC-0	[28]	1	3.33	0.32	39.6	200 × 270	900	4.84	264.5	0.68	312.4	3560	0.111	500	I16	136.0
XSRC-01		1	3.33	0.20	39.6	200 × 270	900	4.84	264.5	0.68	312.4	3560	0.111	500	I16	148.5
XSRC-02		1	3.33	0.32	39.6	200 × 270	900	4.84	264.5	0.68	312.4	3560	0.111	500	I16	158.8
XSRC-03		1	3.33	0.50	39.6	200 × 270	900	4.84	264.5	0.68	312.4	3560	0.111	500	I16	162.6
XSRC-11		0.96	3.33	0.20	39.6	200 × 270	900	4.84	264.5	0.68	312.4	3560	0.111	500	I16	143.1
XSRC-12		0.96	3.33	0.32	39.6	200 × 270	900	4.84	264.5	0.68	312.4	3560	0.111	500	I16	148.4
XSRC-13		0.96	3.33	0.50	39.6	200 × 270	900	4.84	264.5	0.68	312.4	3560	0.111	500	I16	155.5
XSRC-21		0.89	3.33	0.20	39.6	200 × 270	900	4.84	264.5	0.68	312.4	3560	0.111	500	I16	137.5
XSRC-22		0.89	3.33	0.32	39.6	200 × 270	900	4.84	264.5	0.68	312.4	3560	0.111	500	I16	139.9
XSRC-23		0.89	3.33	0.50	39.6	200 × 270	900	4.84	264.5	0.68	312.4	3560	0.111	500	I16	142.2

Note: all columns with fixed-pinned ends.

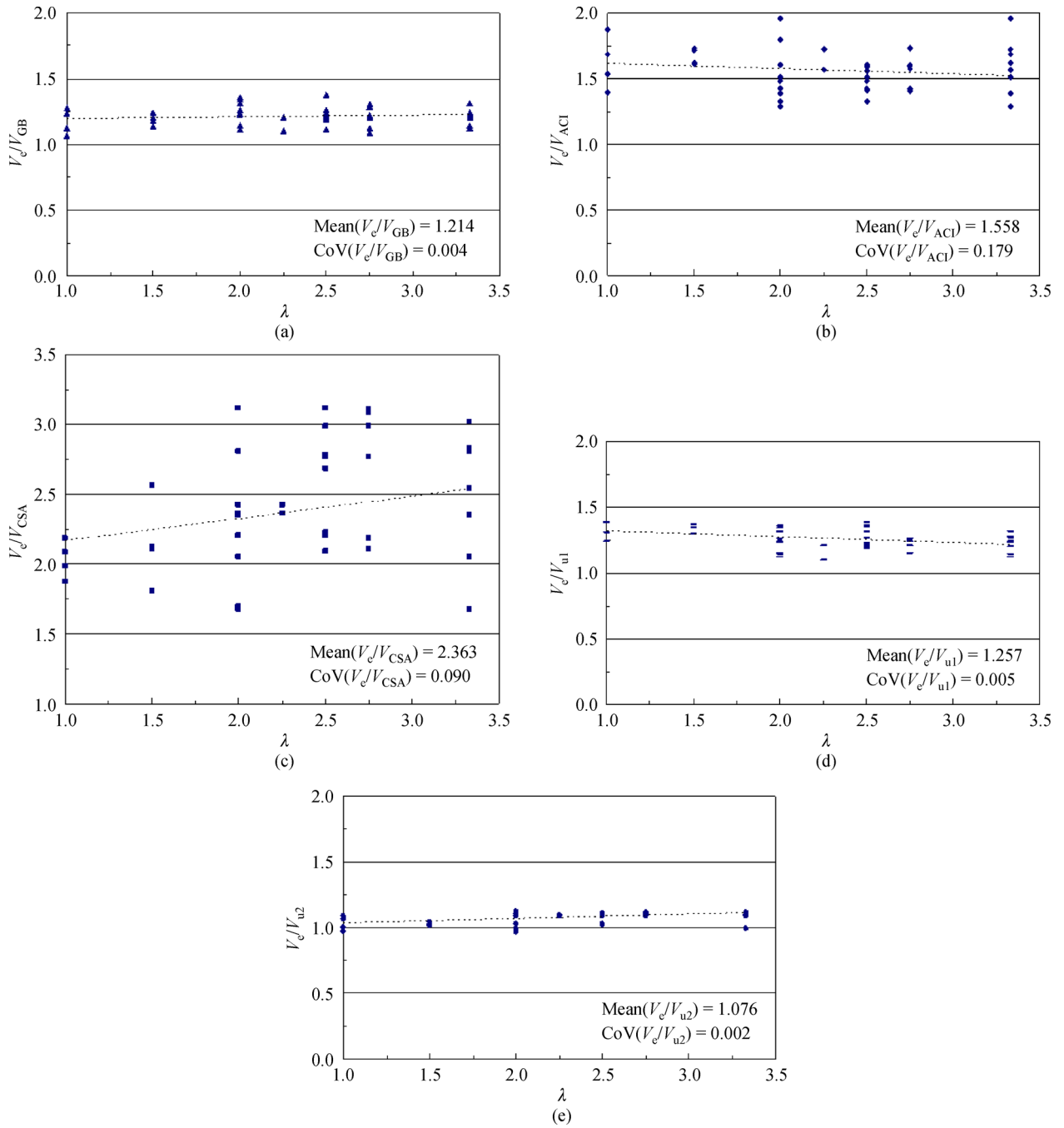


Fig. 8 Variation of measured to calculated strength ratio versus shear span-to-depth ratio. (a) Method in GB 50010-2010; (b) method in ACI 318; (c) method in CSA-04; (d) proposed model of the whole analysis model; (e) proposed model of the three zones analysis model.

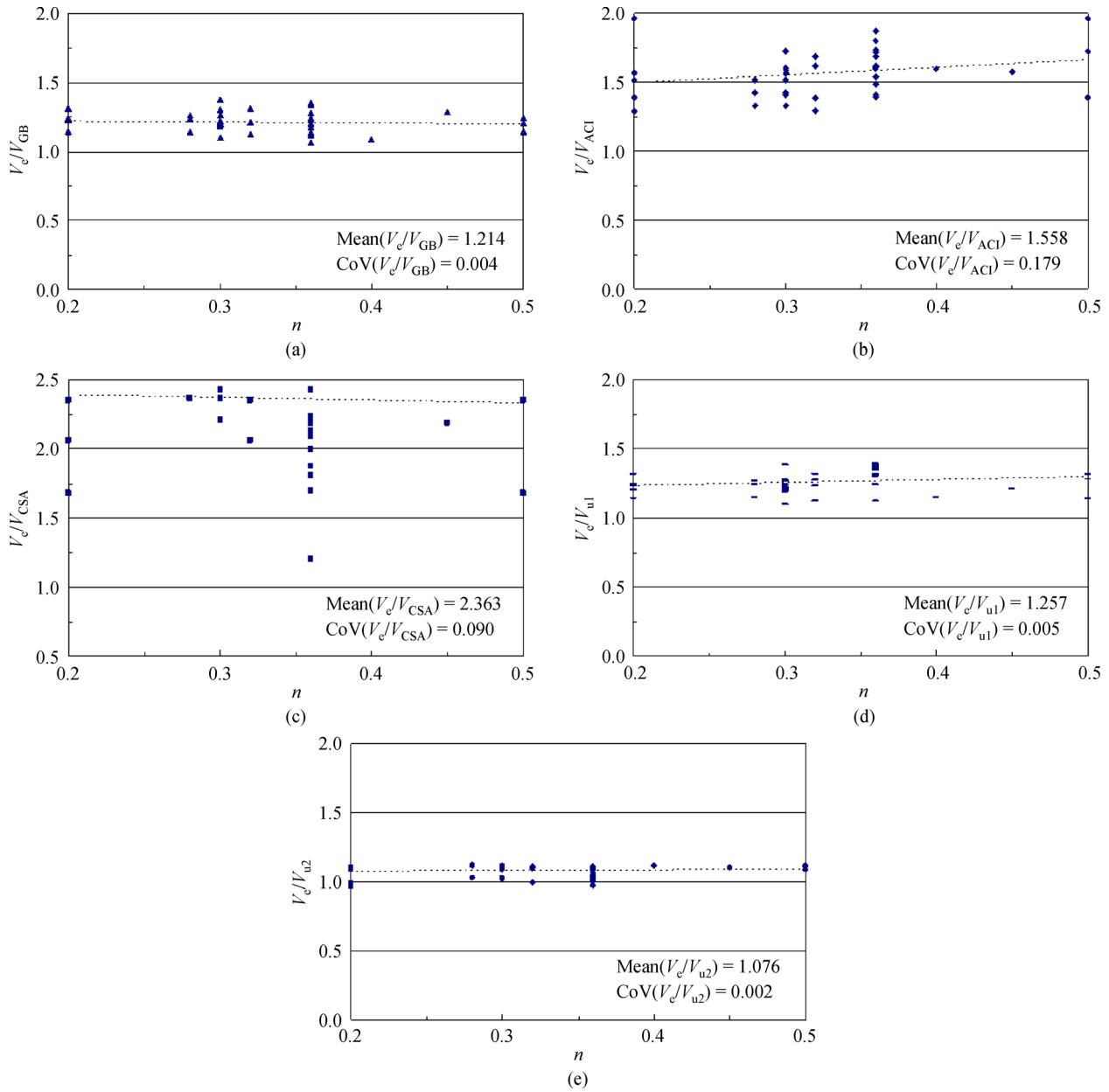


Fig. 9 Variation of measured to calculated strength ratio versus axial-load ratio. (a) Method in GB 50010-2010; (b) method in ACI 318; (c) method in CSA-04; (d) proposed model of the whole analysis model; (e) proposed model of the three zones analysis model.

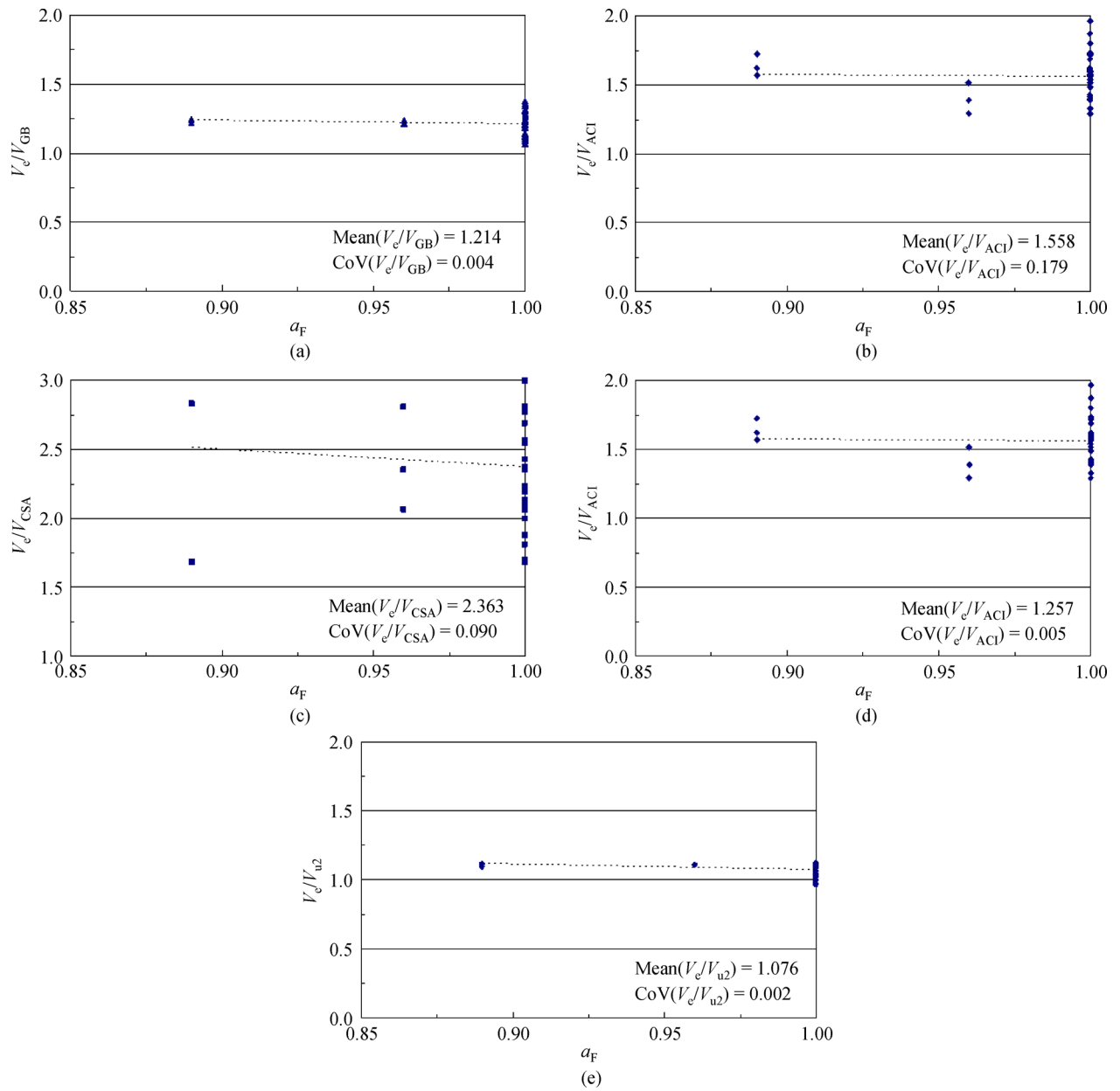


Fig. 10 Variation of strength reduction factor. (a) Method in GB 50010-2010; (b) method in ACI 318; (c) method in CSA-04; (d) proposed model of the whole analysis model; (e) proposed model of the three zones analysis model.

strong correspondence with the test results. The mean ratio of the test value to calculate value shear strength was 1.257 and 1.076, respectively, and its coefficient of variation was 0.005 and 0.002, respectively.

By analyzing the relationship between the experimental value and the calculated value, it was found that the proposed method takes into account the axial-load ratio and the shear span ratio. The shear strength predicted by the proposed three zones analysis model was relatively conservative, especially for columns of small shear span ratios. Comparative results indicated that the shear strength of the GB 50010-2010 model and that of the whole analysis model tended to be safe.

Acknowledgements The experiments by Peng et al. [2] were carried out in the Civil Engineering Experiment Center of Yangtze University, China. This research was funded by the National Natural Science Foundation of China (Grant Nos. 51478048; 51678457), Natural Science Foundation of Hubei Province (Innovation group) of China (No. 2015CFA029) and their support is gratefully acknowledged.

Notation

The following symbols are used in this paper:

A : gross area of section;
 A_1 : core zone area of section;
 A_2 : non core zone area of section;
 a_{CFRP} : CFRP strength reduction factor;
 a_F : the strength reduction factor;
 b : width of column;
 b_f : width of flange of I-beam section;
 b_{st} : width of CFRP;
 D : damage index of specimen;
 D_1 : damage index of the non core zone area of the section column ($D_1 = 0.5$ for moderate damaged and $D_1 = 1$ for severe damaged);
 d_f : thickness of I-beam flange;
 E : elastic modulus of CFRP;
 f_a : yield stress of steel;
 f'_a : yield stress of steel after post-earthquake damage;
 f_c : cylinder strength of concrete;
 f_{ck} : yield stress of longitudinal bars;
 f'_{ck} : yield stress of longitudinal bars after post-earthquake damage;
 f_{st} : tensile stress of CFRP;
 f_{yv} : yield stress of stirrups;
 f'_{yv} : yield stress of stirrups after post-earthquake damage;
 h : height of column;
 h_1 : the high cross section of I-beam;
 l : column height;
 s_{st} : the CFRP spacing;
 t_{st} : the monolayer thickness of CFRP;
 t_w : the thickness of I-beam web;

V_a : shear strength provided by steel;
 V_{a1} : the shear strength of the whole analysis of concrete with RC column section;
 V_{a2} : the shear strength of the RC column consisting of three zones;
 V_c : measured shear strength of column;
 V_i : shear strength provided by arch model;
 α : effective coefficient of arch model;
 β_1 : correlation coefficient;
 β_2 : correlation coefficient;
 λ : shear span ratio;
 n : axial-load ratio;
 ρ_a : steel ratio;
 ρ_l : longitudinal bars ratio;
 ρ_{sv} : stirrups ratio;
 v : the softening coefficient of concrete;
 v_{CFRP} : CFRP strength effective coefficient;
 v_s : shear coefficient of reinforced material;
 σ_c : the oblique compressive stress;
 φ : the angle between the compression concrete and the column axis in the truss model;
 μ : displacement ductility of SRC column at shear failure.

References

- Xu C X, Peng S, Deng J, Wan C. Study on seismic behavior of encased steel jacket-strengthened earthquake-damaged composite steel-concrete columns. *Journal of Building Engineering*, 2018, 17: 154–166
- Peng S, Xu C X, Lu M X, Yang J M. Experimental research and finite element analysis on seismic behavior of CFRP-strengthened seismic-damaged composite steel-concrete frame columns. *Engineering Structures*, 2018, 155: 50–60
- Xu C X, Zeng L, Zhou Q, Tu X, Wu Y. Cyclic performance of concrete-encased composite columns with T-shaped steel sections. *International Journal of Civil Engineering*, 2015, 61: 455–467
- Gholamhoseini A, Khanlou A, MacRae G, Scott A, Hicks S, Leon R. An experimental study on strength and serviceability of reinforced and steel fiber reinforced concrete (SFRC) continuous composite slabs. *Engineering Structures*, 2016, 114: 171–180
- Lampropoulos A P, Paschalis S A, Tsioulou O T, Dritsos S E. Strengthening of reinforced concrete beams using ultra high performance fibre reinforced concrete (UHPFRC). *Engineering Structures*, 2016, 106: 370–384
- Yoo D Y, Banthia N, Yoon Y S. Flexural behavior of ultra-high-performance fiber-reinforced concrete beams reinforced with GFRP and steel rebars. *Engineering Structures*, 2016, 111: 246–262
- Yin S F, Hu K X. Numerical simulation for the pseudo-static test of strengthened RC columns with earthquake-damage based on opensees. *Engineering Structures*, 2015, 31: 145–151
- Kim S H, Choi J H. Repair of earthquake damaged RC columns with stainless steel wire mesh composite. *Advances in Structural*

- Engineering, 2010, 13(2): 393–401
9. Ozbakkaloglu T, Saatcioglu M. Seismic performance of square high-strength concrete columns in FRP stay-in-place formwork. *Journal of Structural Engineering*, 2007, 133(1): 44–56
 10. Ozbakkaloglu T, Saatcioglu M. Seismic behavior of high-strength concrete columns confined by fiber reinforced polymer tubes. *Journal of Composites for Construction*, 2006, 10(6): 538–549
 11. Idris Y, Ozbakkaloglu T. Behavior of square fiber reinforced polymer-high-strength concrete-steel double-skin tubular columns under combined axial compression and reversed-cyclic lateral loading. *Engineering Structures*, 2016, 118: 307–319
 12. Idris Y, Ozbakkaloglu T. Seismic behavior of high-strength concrete-filled FRP tube columns. *Journal of Composites for Construction*, 2013, 17(6): 04013013
 13. Idris Y, Ozbakkaloglu T. Seismic behavior of FRP-high-strength concrete-steel double skin tubular columns. *Journal of Structural Engineering*, 2012, 140: 1299–1328
 14. Ozbakkaloglu T, Lim J C. Axial compressive behavior of FRP-confined concrete: Experimental test database and a new design-oriented model. *Composites. Part B, Engineering*, 2013, 55: 607–634
 15. Ozbakkaloglu T, Jian C L. Confinement model for FRP-confined high-strength concrete. *Journal of Composites for Construction*, 2013, 18: 2537–2547
 16. Fukuyama K, Higashibata Y, Miyauchi Y. Studies on repair and strengthening methods of damaged reinforced concrete columns. *Cement and Concrete Composites*, 2000, 22(1): 81–88
 17. Cai W D. Experimental study on seismic behavior for reinforced concrete short column strengthened with carbon fiber sheet. Thesis for the Master's Degree. Tianjin: Tianjin University, 2001 (in Chinese)
 18. Iacobucci R D, Sheikh S A, Bayrak O. Retrofit of square concrete columns with carbon fiber-reinforced polymer for seismic resistance. *ACI Structural Journal*, 2003, 100(6): 785–794
 19. Sezen H, Moehle J P. Shear strength model for lightly reinforced concrete columns. *Journal of Structural Engineering*, 2004, 130(11): 1692–1703
 20. Wang X L, Fan J W, Wang H. Experimental study on the damaged RC frame structure strengthened with CFRP under low-cycle repeated load. *World Earthquake Engineering*, 2009, 25(3): 119–123 (in Chinese)
 21. Wang J L. Experimental Research on Seismic Behaviors of Earthquake-damaged Concrete Columns Restrengthened with CFRP. Thesis for the Master's Degree. Nanjing: Southeast University, 2009 (in Chinese)
 22. Zhao S H, Ye L P. Shear strength analysis of concrete column retrofitted with CFRP sheet based on strut-arch model. *Engineering Mechanics*, 2001, 18(6): 134–140
 23. Zhang Y, Cui X G, Yang D, Li X B. Experimental investigation on the seismic behaviors of repaired seriously damaged reinforced concrete columns. *Industrial Construction*, 2011, 41(7): 38–44 (in Chinese)
 24. Zhou C D, Tian T, Lv X L, Bai X B, Li H. Test study on seismic performance of pre-damaged RC Cylinder piers strengthened with pre-stressed FRP belts. *Journal of The China Railway Society*, 2012, 34(10): 103–114 (in Chinese)
 25. Pan Z F, Li B. Truss-arch model for shear strength of shear-critical reinforced concrete columns. *Journal of Structural Engineering*, 2013, 139(4): 548–560
 26. Jin C H, Pan Z F, Meng S P, Qiao Z. Seismic behavior of shear-critical reinforced high-strength concrete columns. *Journal of Structural Engineering*, 2015, 141(8): 04014198
 27. Ichinose T. A shear design equation for ductile RC members. *Earthquake Engineering & Structural Dynamics*, 1992, 21(3): 197–214
 28. Yang J M. Finite element analysis on seismic performance of repaired and strengthened seismic-damaged steel reinforced concrete frame columns. Thesis for the Master's Degree. Wuhan: Wuhan University of Science and Technology, 2017 (in Chinese)
 29. Liu J D. Research on modeling of hysteretic characteristics of RC frames damaged during earthquake. Thesis for the Master's Degree. Chongqing: Chongqing University, 2015 (in Chinese)
 30. Wang B, Zheng S S, Guo X F, Yu F, Zhang H R. Seismic damage analysis for SRHSHPC frame columns. *Engineering Mechanics*, 2012, 29(2): 61–68
 31. Zhao G T, Cao F B. Seismic behavior of reinforced concrete crack-short columns strengthened with CFRP. *Earthquake Resistant Engineering and Retrofitting*, 2010, 32(5): 85–90 (in Chinese)
 32. Lu M X. Experimental research on seismic behavior of CFRP-strengthened seismic-damaged SRC columns. Thesis for the Master's Degree. Jingzhou: Yangtze University, 2017 (in Chinese)
 33. Wan C. Experimental study on steel reinforced concrete frame columns strengthened with steel angles and strips damaged by simulated earthquake. Thesis for the Master's Degree. Jingzhou: Yangtze University, 2017 (in Chinese)
 34. Zhang Y F. Experimental research on the seismic performance of damaged reinforced concrete columns strengthened with carbon fiber reinforced plastics. Thesis for the Master's Degree. Baotou: Mongolia University of Science and Technology, 2009 (in Chinese)
 35. GB50010-2010. Code for Design of Concrete Structures. China Architecture & Building Press, 2010 (in Chinese)
 36. Wei J P, Zhang X H. Analysis on the shear bearing capacity of solid-webbed steel reinforced concrete short column based on trussed arch model. *Progress in Steel Building Structures*, 2011, 13(4): 52–56 (in Chinese)
 37. Ye L P, Zhao S H, Li Q W, Yu Q R, Zhang K. Calculation of shear strength of concrete column strengthened with carbon fiber reinforced plastic sheet. *Journal of Building Structures*, 2000, 21(2): 59–67
 38. ACI Committee 318. Building code requirements for structural concrete (ACI 318-05) and commentary (ACI 318R-05). American Concrete Institute, 2005
 39. CSA A23.3-04. Design of concrete structures. Canadian Standards Association, 2004